Coupling of thermal and mass diffusion in regular binary thermal lattice gases

Ronald Blaak*
Grupo Interdisciplinar de Sistemas Complicados (GISC), Departamento de Matemáticas, Universidad Carlos III de Madrid, Avenida de la Universidad 30, 28911 Leganés, Madrid, Spain

David Dubbeldam†
Department of Chemical Engineering, University of Amsterdam, Nieuwe Achtergracht 166, 1018 WV Amsterdam, The Netherlands
(Received 8 May 2001; published 20 November 2001)

We have constructed a regular binary thermal lattice gas model in which the thermal diffusion and mass diffusion are coupled and form two nonpropagating diffusive modes. The power spectrum is shown to be similar in structure as for the one in real fluids, in which the central peak becomes a combination of coupled entropy and concentration contributions. Our theoretical findings for the power spectra are confirmed by computer simulations performed on this model.

DOI: 10.1103/PhysRevE.64.062102 PACS number(s): 05.20.Dd, 05.50.+q, 05.60.−k

The power spectrum of light scattered by a binary solution is more complicated than that of a single component fluid. The central peak contains combined effects of entropy and concentration fluctuations [1,2]. The cross effects are well known in nonequilibrium thermodynamics as the Dufour effect and the Soret effect, and are caused by the coupling between heat flow and diffusion. For example, heat may be transported by conduction but also by diffusion of the two components. In the simplified two-dimensional model presented here this coupling phenomena can be analyzed in detail.

Lattice gas automata (LGA) are plagued by many defects. Although some of these defects can be removed, the models are, in general, not suitable for modeling realistic fluids because they do not exhibit a fully realistic thermodynamical behavior. They are, however, useful tools for understanding more fundamental problems in thermodynamics related to discretization and testing concepts in statistical mechanics [3]. In LGA, the positions and velocities of pointlike particles are discretized onto a lattice [4]. The dynamics consist of a cyclic process of propagating particles according to their velocity to a neighboring node followed by local collisions that typically conserve mass and momentum.

In order to recover the macroscopically isotropic Navier-Stokes equations the lattice in two-dimensions is usually chosen to be hexagonal. Apart from problems related to this, early LGA were also plagued by unwanted spurious invariants [5–7]. A satisfactory extension to include thermal properties in LGA was made by Grosfils, Boon, and Lallemand (GBL), who introduced a multiple speed model, defined on a two-dimensional hexagonal lattice [8]. The model uses a velocity set consisting of a single rest particle and three rings, each containing six directions, with velocities of magnitude 1, $\sqrt{3}$, and 2.

Generalizations of LGA to mixtures have been used to study interfaces and phase transitions [9]. Some of these models use a passive label to distinguish the different species [10]. In other models the particles live on different lattices [11,12]. However, these models are athermal and do not show the coupling phenomena we are interested in. A two species thermal model by using a passive label, is also not suitable, because mass and heat transport would completely decouple [13].

Here we introduce a thermal binary lattice gas model capable of capturing the essence of a real mixture with respect to coupling of entropy and concentration fluctuations. This model allows us to calculate the coupling quantitatively and separate the different contributions, which in the continuous case in general is only possible in the low-density limit. The two species of particles live on separate two-dimensional hexagonal lattices and are labeled red and blue. Independently they would behave as normal GBL models, but we allow the particles to interact during the collision phase, i.e., momentum and/or energy can be transferred from one to the other lattice. The number of red and blue particles, however, is constant in every collision.

The state of a node can be specified by a set of Boolean occupation numbers $n_{i\mu}$, denoting the presence or absence of a particle of type $\mu=\{r,b\}$ in velocity channel c_i, where i is a label running over all 19 velocities. Due to the Boolean nature of LGA, the ensemble average of the occupation numbers $f_{i\mu}$ in equilibrium, is described by a Fermi-Dirac distribution

$$f_{i\mu}\equiv\langle n_{i\mu}\rangle=\frac{1}{1+\exp[-\alpha_\mu+\beta\boldsymbol{c}_i^2/2-\boldsymbol{\gamma}\cdot\boldsymbol{c}_i]}, \qquad (1)$$

where α_r, α_b, β, and $\boldsymbol{\gamma}$ are Lagrange multipliers. Here, β is the inverse temperature, α_r and α_b fulfill a chemical potential role, and $\boldsymbol{\gamma}$ is a parameter conjugate to the flow velocity. For simplicity, we will work in the overall zero momentum case by setting $\boldsymbol{\gamma}=0$.

A collision outcome is chosen with equal probability amongst all members of an *equivalence class*, i.e., a group of states having the same red mass, blue mass, total momentum, and total energy. In a *regular binary mixture* at most two particles, each of different type, can be in the same velocity

*Electronic address: rblaak@pa.uc3m.es
†Electronic address: dubbeldam@its.chem.uva.nl

state [14]. This differs from the *color mixture* where the particles of the original single specie model are given a color to distinguish between them and was analyzed in the case of the GBL color mixture (CGBL) [13]. In that case the collision operator could be eqnarray into two separated steps: a GBL collision and an independent redistribution of the colors, which made the simulations a relative simple extension of normal GBL simulations, even though the number of different states in the CGBL model was 3^{19}. Here we have a ''true'' 38-bit model leading to 2^{38} states on which the collision operator has to act. Clearly a naive lookup-table strategy in order to simulate this system is only feasible if the table is constructed partially and stored temporarily during the simulations, due to the excessive memory requirements for storing the complete table.

Regular binary mixtures, however, do allow for a convenient solution, which is less efficient than storing the complete collision table, but has still a relative good performance (about a factor 2–5 slower than CGBL). Rather than storing a collision table based on the states, we make one based on the different classes. This allows us to generate a set of outgoing classes for the two species and via a GBL-like process an outgoing state. If this is combined with the 48 symmetry operations (six rotations, two reflections, red/blue symmetry, and particle/hole symmetry), we get a working algorithm that can be used on a computer with 256 MB of memory [15].

The theoretical framework for thermal lattice gases is well established [16], and is here extended to binary mixtures. It is possible to solve the many-body dynamics of LGA by using the Boltzmann molecular chaos assumption. Although one would expect deviations for higher densities, it turns out that these deviations are very small, in fact for many purposes even within a few percent accuracy. Therefore, provided the fluctuations in the average occupation numbers are small, a Taylor expansion of the collision term in the neighborhood of the equilibrium distribution is justified, yielding a linearized collision operator Ω. Then, in first approximation the behavior of the system can be obtained by analyzing these deviations in terms of eigenmodes.

In the analysis of the behavior of fluctuations in LGA mixtures it is convenient to introduce the colored scalar inproduct [13,17]

$$\langle A|B\rangle = \sum_{i\mu} A(\boldsymbol{c}_{i\mu})B(\boldsymbol{c}_{i\mu})\kappa_{i\mu}, \tag{2}$$

where $\kappa_{i\mu}=f_{i\mu}(1-f_{i\mu})$ is the variance in the average occupation number. For reasons of symmetry κ is included in definition of the right vectors, i.e. $|B\rangle_{i\mu}=\kappa_{i\mu}B(\boldsymbol{c}_{i\mu})$.

Following the method of Résibois and Leener [18] we need to find the $\boldsymbol{k}$-dependent eigenfunctions and eigenvalues of the single-time step Boltzmann propagator

$$e^{-\imath\boldsymbol{k}\cdot\boldsymbol{c}}(1+\Omega)|\psi(\boldsymbol{k})\rangle = e^{z(\boldsymbol{k})}|\psi(\boldsymbol{k})\rangle. \tag{3}$$

Within this formulation the hydrodynamic modes are characterized by the fact that the eigenvalues z_μ should go to zero in the limit of small wave vectors. Therefore, we can derive these $\boldsymbol{k}$-dependent eigenvectors and eigenvalues by making a Taylor expansion in $\boldsymbol{k}$. The resulting eigenvalues to second order in $\boldsymbol{k}$ are given by

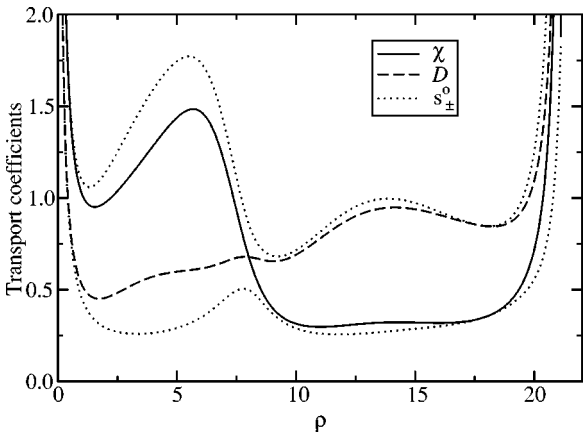

FIG. 1. The diffusive transport values as a function of the density at reduced temperature $\theta=0.1$ and fraction of red particles $P_r=0.9$.

$$z_\pm(\boldsymbol{k}) = \pm\imath c_s\boldsymbol{k} - \Gamma\boldsymbol{k}^2, \tag{4}$$

$$z_\perp(\boldsymbol{k}) = -\nu\boldsymbol{k}^2, \tag{5}$$

$$z_{s_\pm}(\boldsymbol{k}) = -s^o_\pm\boldsymbol{k}^2. \tag{6}$$

It is with these modes that the binary-mixture responds to deviations from thermal equilibrium. The first two eigenmodes describe sound propagating (in opposite directions parallel to $\boldsymbol{k}$) with Γ the sound damping coefficient and c_s the adiabatic sound speed. The third eigenvalue describes a shear mode with ν the shear viscosity coefficient. The last two eigenvalues represent purely diffusive, nonpropagating processes, but are in general not directly related to a familiar transport coefficient. Rather they always appear in combination with each other and can be expressed in other transport properties by

$$s^o_\pm = \frac{1}{2}(\chi+\mathcal{D}) \pm \frac{1}{2}\sqrt{4Q^2+(\chi-\mathcal{D})^2}, \tag{7}$$

where χ is the generalized thermal diffusivity, $\mathcal{D}$ a property related to the mass diffusion, and Q can be considered as a measure of the correlation between the two. Another interesting relation can be obtained by introducing the ratio of the specific heats γ

$$\Gamma = \frac{1}{2}[\nu+(\gamma-1)\chi]. \tag{8}$$

In Fig. 1 the diffusive transport properties are shown at fixed reduced temperature $\theta=\exp(-\frac{1}{2}\beta)$. The modes $s^o_\pm$ converge for low densities to the thermal diffusivity and mass diffusion, due to the decoupling of the fluctuations in entropy and energy. This behavior resembles the situation for binary solutions where a formula similar to Eq. (7) exists [2], with the same decoupling in the very dilute limit. In our model

this means that the ratio $Q/(\chi-\mathcal{D})$ vanishes. The value of Q, however, will in general remain small but finite due to the divergencies of the transport coefficients in the low-density limit of LGA.

The decoupling is also observed in the limit of a single specie, i.e., the fraction of blue particles P_b goes to zero. In this limit the model reduces to a normal GBL model, albeit that the diffusion related property $\mathcal{D}$ will remain finite. For reasons of symmetry $s_{\pm}^{o}$ also converge to χ and $\mathcal{D}$ in the limit of equal red and blue density. In fact this special limit can be analyzed completely in a similar way as done for CGBL [13]. Finally decoupling appears in two other cases due to the duality of the model under interchanging particles and holes, these are the high-density limit and the limit in which one of the sublattices is almost completely filled.

The decoupling arises from an effective equipartition in the model making the ratio of the average occupation numbers f_{ir}/f_{ib} the same constant for each velocity channel i. As can be seen in Fig. 1 there seem to be also intermediate values at which decoupling appears. Although indeed the $s_{\pm}^{o}$ converge to χ and $\mathcal{D}$ this is not due to decoupling via equipartition but due to the cancellation of terms. This property could obviously be used in the analysis, but the location of these points depends in a nontrivial way on the chosen system parameters.

The Boltzmann approximation enables us to calculate the modes up to fairly large wave vectors, even within the generalized hydrodynamic regime. In the hydrodynamical regime of small wave vectors $\boldsymbol{k}$, small frequencies ω, the hydrodynamical modes are well separated from the kinetic modes that, due to their exponential decay, can be neglected. In combination with a Taylor expansion, this allows one to derive a Landau-Placzek approximation of the spectral density $S(\boldsymbol{k},\omega)$,

$$\frac{S(\boldsymbol{k},\omega)}{S(\boldsymbol{k})}=\sum_{\pm}\frac{\gamma-1}{\gamma}\left(1\pm\frac{\chi-\mathcal{D}}{s_{+}^{o}-s_{-}^{o}}\right)\frac{s_{\pm}^{o}k^{2}}{\omega^{2}+(s_{\pm}^{o}k^{2})^{2}}+\sum_{\pm}\frac{1}{\gamma}\frac{\Gamma k^{2}}{(\omega\pm c_{s}k)^{2}+(\Gamma k^{2})^{2}}+\frac{1}{\gamma}[\Gamma+(\gamma-1)\chi]\times\frac{k}{c_{s}}\sum_{\pm}\frac{c_{s}k\pm\omega}{(\omega\pm c_{s}k)^{2}+(\Gamma k^{2})^{2}},\tag{9}$$

where $S(\boldsymbol{k})$ is the static structure factor.

The spectrum contains an unshifted central peak and is formed by two Lorentzians due to the nonpropagating processes characterized by $s_{\pm}^{o}$. The shear mode does not contribute to the spectrum and the two propagating modes lead to the presence of the two frequency-shifted Brillouin lines. The last two terms in Eq. (9) have a contribution orders of magnitude smaller than the amplitude of the Lorentzians and induce a slight pulling of the peaks towards the central peak [2]. The symmetry of the different contributions is such that the ratio of the integrated contributions of the central peak and the Brillouin components is constant and given by $\gamma-1$.

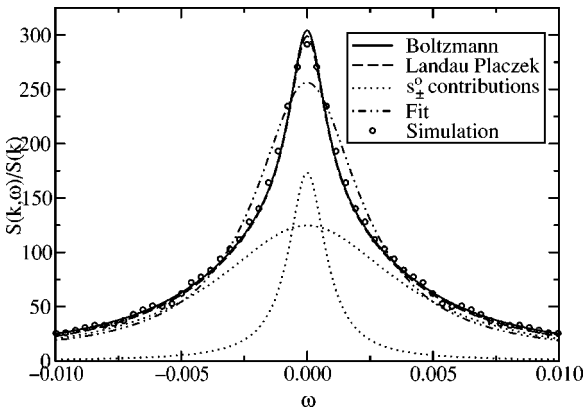

FIG. 2. The central part of the spectrum in the Boltzmann approximation, the Landau-Placzek approximation, the $s_{\pm}^{o}$ contributions are shown separately. The system parameters are $\theta=0.1$, $\rho=6.5$, $P_r=0.05$, $k_x=4\times2\pi/512$. The wave vector $\boldsymbol{k}$ and frequency ω are given in reciprocal lattice and time units, respectively.

Figure 2 illustrates the composition of the central peak. The simulation results overlap perfectly with the Boltzmann and Landau-Placzek approximations. The contributions of the diffusive modes to the central peak are indicated separately and for comparison a least square fit based on Eq. (9) to the whole spectrum, including the Brillouin peaks outside the interval shown, is made based on approximating the central peak by a single Lorentz.

As can be seen from the Landau-Placzek expression (9) one of these contributions will vanish in the limits where $s_{\pm}^{o}$ converge to χ and $\mathcal{D}$ and the central peak reduces to

$$\frac{S^{\mathrm{cen}}(\boldsymbol{k},\omega)}{S(\boldsymbol{k})}=\frac{\gamma-1}{\gamma}\frac{2\chi k^{2}}{\omega^{2}+(\chi k^{2})^{2}},\tag{10}$$

even though the other transport coefficient remains finite. As mentioned before, this occurs at a limited set of locations, such as the low/high-density limit, single specie limits, and the limit of equal red and blue density. In addition to these general limits it is also found in the low/high-temperature regions close to densities where all rings of particles with the same absolute velocity are completely filled or empty [13]. This reduction of the central peak to a single Lorentz in the low-density limit is also found in the very dilute limit of binary solutions. But contrary to what is found here, it is usually the thermal diffusivity that disappears [1,2].

If $s_{\pm}^{o}$ are sufficiently different, one can separate the two contributions in the spectrum outside the limits mentioned above (Fig. 2). This does not automatically imply that one could obtain the transport values of interest from the experimental spectrum only, because they can still differ significantly from χ and $\mathcal{D}$.

In the low-density limit we can identify $\mathcal{D}$ with the mass diffusion of the GBL model. In the limit of a single specie this is no longer true if one goes to higher densities, even though all other properties converge to their GBL values. The origin of this problem is found in the possibility to have more than one particle with the same velocity in this model. Continuous theory suggests that $\mathcal{D}$ is not the correct gener-

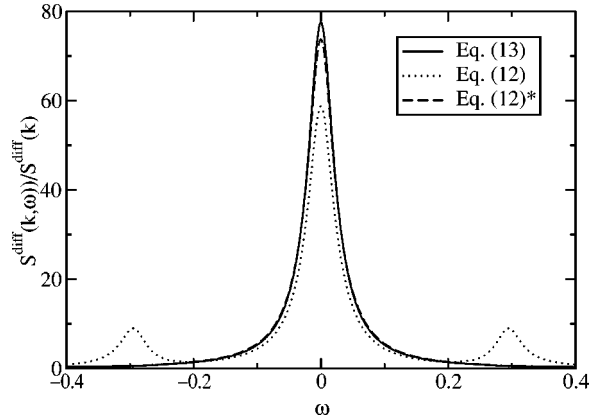

FIG. 3. A diffusive spectrum based on the different possible choices for the density difference. The curve labeled by an asterisk is corrected by subtracting the propagating part. The system parameters are $\theta=0.05$, $\rho=10.0$, $\rho_r/\rho=0.15$, $k_x=20\times 2\pi/512$. The wave vector $\boldsymbol{k}$ and frequency ω are given in reciprocal lattice and time units, respectively.

alization of the diffusion [2]. This is consistent with the way in which this quantity arises in the present model [15].

The proper generalization of the diffusion is not completely trivial. There is some ambiguity in the choice one needs to make. In a continuous fluid one would consider the decay of a signal of the type

$$|\mathrm{diff}\rangle = \frac{|R\rangle}{P_r} - \frac{|B\rangle}{P_b}, \tag{11}$$

where $|R\rangle_{i\mu}=\delta_{r\mu}$ and $|B\rangle_{i\mu}=\delta_{b\mu}$. A spectrum based on this normalized density difference, however, leads to Brillouin peaks as is shown in Fig. 3. This was already indicated earlier in an athermal binary mixture [14], where it was proposed to use

$$|\mathrm{diff}\rangle = \frac{|R\rangle}{\langle R|R\rangle} - \frac{|B\rangle}{\langle B|B\rangle}. \tag{12}$$

But in the thermal case this signal suffers from the same problem. In both cases one could, in principle, extract the propagating part, but it is more natural to reformulate the density of interest to

$$|\mathrm{diff}\rangle = \frac{|R\rangle}{\langle p|R\rangle} - \frac{|B\rangle}{\langle p|B\rangle}, \tag{13}$$

with $p=c^2/2$ being the energy per particle. This problem originates from the lack of equipartition, but in general the differences between the various choices will remain small [15].

In conclusion, we presented a thermal binary mixture, which exhibits spontaneous thermal and concentration fluctuations. The regular mixture model is much more involved than the color mixture, but it is closer to the dynamics of real binary mixtures, as it is able to capture the coupling phenomena observed in binary solutions. The coupling between energy transport and diffusion results in two diffusive nonpropagating modes and in a more complicated structure of the power spectrum. In general, however, these two ''true'' transport coefficients do not seem to correspond with a conventional transport coefficient, but always appear in combination with each other.

The LGA spectrum is similar in structure as the one for the continuous case. In general, it is impossible to separate the entropy and concentration contributions, and the central peak can not be described by a single Lorentzian. However, in several limits, namely, the low/high-density limit, the single specie limit, and the equal red/blue limit, the true modes $s_{\pm}^{o}$ converge to generalized thermal diffusivity χ and a mass diffusion like $\mathcal{D}$. In other cases the different transport coefficients can be determined by using the theoretical framework, that provides an accurate description as is demonstrated by the comparison of the Landau-Placzek expression with simulation results.

The authors would like to thank H. Bussemaker and D. Frenkel for helpful discussions. R.B. acknowledges the financial support of the EU (Contract No. HPMF-CT-1999-00100).

[1] R.D. Mountain and J.M. Deutch, J. Chem. Phys. **50**, 1103 (1969).
[2] J.P. Boon and S. Yip, *Molecular Hydrodynamics* (McGraw-Hill, New York, 1980).
[3] J.P. Rivet and J.P. Boon, *Lattice Gas Hydrodynamics*, Cambridge Nonlinear Science Number 11 (Cambridge University Press, Cambridge, 2001).
[4] U. Frisch, B. Hasslacher, and Y. Pomeau, Phys. Rev. Lett. **56**, 1505 (1986).
[5] R. Brito, M.H. Ernst, and T.R. Kirkpatrick, J. Stat. Phys. **62**, 283 (1991).
[6] S.P. Das and M.H. Ernst, Physica A **187**, 191 (1992).
[7] M.H. Ernst and S.P. Das, J. Stat. Phys. **66**, 465 (1992).
[8] P. Grosfils, J.-P. Boon, and P. Lallemand, Phys. Rev. Lett. **68**, 1077 (1992).
[9] D.H. Rothman, Rev. Mod. Phys. **66**, 1417 (1994).
[10] H. Chen and W.H. Matthaeus, Phys. Fluids **30**, 1235 (1987).
[11] D. Dab, J.-P. Boon, and Y.-X. Li, Phys. Rev. Lett. **66**, 2535 (1991).
[12] R. Kapral, A. Lawniczak, and P. Masiar, Phys. Rev. Lett. **66**, 2539 (1991).
[13] R. Blaak and D. Dubbeldam, Phys. Rev. E **63**, 021109 (2001).
[14] M.H. Ernst and J.W. Dufty, J. Stat. Phys. **58**, 57 (1990).
[15] R. Blaak and D. Dubbeldam (unpublished).
[16] P. Grosfils, J.-P. Boon, R. Brito, and M.H. Ernst, Phys. Rev. E **48**, 2655 (1993).
[17] D. Hanon and J.P. Boon, Phys. Rev. E **56**, 6331 (1997).
[18] P. Résibois and M. de Leener, *Classical Kinetic Theory of Fluids* (Wiley, New York, 1977).